

The effect of preadsorbed K on the size distribution of Au nanoparticles on TiO₂(1 1 0) surface

A.M. Kiss^a, M. Švec^b, A. Berkó^{a,*}

^a Reaction Kinetics Research Group of the Hungarian Academy of Sciences, University of Szeged, P.O. Box 168, H-6701 Szeged, Hungary

^b Department of Thin Films, Institute of Physics of the Czech Academy of Sciences, Prague, Czech Republic

Received 24 March 2006; accepted for publication 21 June 2006

Available online 28 July 2006

Abstract

The effect of K on the morphology of Au nanoparticles deposited on TiO₂(1 1 0) surface is investigated by STM-STS and AES methods. For comparison, the enhanced concentration of oxygen defect sites generated by Ar⁺ bombardment was also studied. It was found that both the K additive and the oxygen defect sites induce a pronounced decrease in the average size of the Au nanoparticles evolved at 320 K. On the clean TiO₂(1 1 0) the average size of Au particles is 4.3 nm at approximately monolayer coverage of gold, while in the presence of K or oxygen vacancies this value decreased to 2.5 nm. In spite of the reduced average diameter detected at room temperature, the mean size of the Au nanoparticles increased significantly from 2.5 nm up to 7 nm on the effect of annealing at 500–700 K for K pre-coverages of 0.3–1 ML. For the clean and the Ar⁺ pretreated TiO₂(1 1 0) surfaces the mean size of the Au particles changed only slightly on the effect of the same thermal treatments.

© 2006 Elsevier B.V. All rights reserved.

Keywords: Au nanoparticles; TiO₂(1 1 0) support; Influence of K additive; Metal vapour deposition, MVD; Scanning tunnelling microscopy, STM; Size-control of the metal nanoparticles

1. Introduction

Since the finding of low temperature oxidation of CO on supported Au catalysts, a tremendous research work has been made for the detailed understanding of this reaction and for the development of effective catalysts for different applications, like the purification of hydrogen or improved removal of CO contaminant from exhaust gases [1–5]. As a bulk gold is practically inert, however, in the form of oxide-supported nanoparticles it shows high activity in several oxidation reactions even at room temperature. The deep insight into this behaviour is a great challenge standing ahead of the surface science community. Different factors are thought to play important role in this phenomenon: (i) special chemistry at the perimeter of Au nanoparticles; (ii) a marked role of the low coordinated metal atoms of high

surface density for the small particles; (iii) modified electronic structure caused by the size-reduction (electron confinement); (iv) electric charging of Au particles caused by the charge transfer from/to the support [5–7].

The general properties of metal/oxide interfaces – especially of metal/TiO₂(rutile) systems – were substantially characterized in the last decade both on polycrystalline and 2D model systems [8–10]. Au belongs to the group of so called non-reactive admetals for which the oxidation state of Ti⁴⁺ ions does not change on the effect of bonding of the given metal to the support and the growing of the adlayer follows mainly Volmer–Weber (3D growth mode) mechanism. Even in these cases, however, the different surface defect sites can play an important role in the formation (size, morphology and lateral distribution) of admetal nanoparticles [11–18]. It is worth mentioning that the initial surface morphology before some reaction can naturally change during the reaction or the treatments at higher pressures of the reactant gases. For example, the annealing of

* Corresponding author. Tel.: +36 62 544 646; fax: +36 62 420 678.
E-mail address: aberko@chem.u-szeged.hu (A. Berkó).

Au-covered TiO₂(110) surfaces in oxygen ambient (from 10⁻⁴ mbar to 1 bar) has shown a significant increase in the particle size, especially at higher temperatures [11,12]. The recent studies reported by Lee et al. have shown that the deposition of ionic gold clusters of small sizes (<1 nm) results in a nanoparticle array with unexpected sintering resistance and the system possesses very high activity towards low temperature CO oxidation [19,20]. All of these observations claim for further detailed studies in which the tailoring of the Au crystallites is achieved.

In contrast to gold, potassium belongs to the so called reactive admetals on TiO₂ substrate where the formation of strong K–O bond can be clearly detected by XPS, UPS and SEXAFS measurements [21–27]. Although a complete charge transfer was assumed between K(4s) and Ti(3d) orbitals resulting in the reduction of Ti⁴⁺ into Ti³⁺, the clear detection of this latter species failed and this phenomenon was explained by the delocalization of the transferred charge among the adjacent Ti ions [25]. The formation of potassium oxides was concluded from the appearance of additional vibrational modes detected by HREELS and evidenced also by UPS spectra of the valence band region [24]. These experimentally observed features were well explained by theoretical calculations, too [25,28,29].

In the present work the effect of the predeposition of K is studied on the formation and thermal stability of Au nanoclusters on TiO₂(110) surface mainly by scanning tunnelling microscopy (STM). For comparison, the effect of Ar⁺ bombardment also was investigated.

2. Experimental

The experiments were carried out in an UHV chamber equipped with a room temperature scanning tunnelling microscope (WA-Technology), a cylindrical mirror analyser (STAIB) applied for Auger-electron spectroscopy (AES) and a quadrupole mass spectrometer (BALZERS) for gas analysis (MS).

TiO₂(110) single crystal was directly fixed to a Ta filament by an oxide adhesive (ceramobond 571, AREMCO Products) and mounted on a transferable sample holder. The probe was annealed by current flowing through the Ta filament and the temperature was measured by a chromel–alumel (K-type) thermocouple stuck to the side of the sample. An initial cleaning procedure was started by a gradual increase of the temperature up to 1100 K and continued by several hours of Ar⁺ bombardment at stepwise decreased ion energy of 2 keV, 1.5 keV and 1 keV (4–6 μA cm⁻²) at 1100 K. This procedure resulted in not only the purification of the sample (mainly from Ca contamination) but also caused some reduction in the subsurface layers and made it possible to avoid the charging problems during the spectroscopic and microscopic measurements. From time to time (after extended use of the sample) the surface was reoxidized in 5 × 10⁻⁴ mbar oxygen for 10 min at 900 K. The final treatment was usually a short

annealing at 1100 K in UHV. The surface of the TiO₂(110) probe obtained in this way exhibited mainly (1 × 1) ordered phase accompanied by some (3–5% of the total surface area) outrising dots and 1D strings in the [001] orientation [30].

The chemical cleanness of the sample and the metal overlayer were checked by Auger-electron spectroscopy and the surface morphology was verified by scanning tunnelling microscopy. The Au and K coverages are expressed in monolayer equivalent (ML), which corresponds to 1.39 × 10¹⁵ Au-atom cm⁻² (taking into account the atom density of an Au(111) surface) and ca. 5 × 10¹⁴ K-atom cm⁻² (by ordering one K atom to each unit cell of the support lattice), respectively [27]. In the case of gold, the actual coverage was calculated by determining of the total volume of the well separated 3D metal nanoparticles formed on the effect of annealing at 700 K. The coverage of K was calibrated by taking into account that the temperature of the adsorption (app. 330 K) was not low enough for the formation of K multilayer, accordingly, the saturation of the relative intensities of the AES peaks (K_{252 eV} and Ti_{385 eV}) indicates the filling of the first K-layer.

For STM imaging chemically etched W-tips were applied and sharpened “in situ” above the TiO₂ surface by applying 5–10 V pulses. Typical tunnelling parameters of +1.5 V (referenced to the surface) and 0.2 nA were used for the imaging of both the clean and Au-covered TiO₂(110) surfaces. In the presence of surface potassium a slightly increased bias (2–3 V) was applied due to the higher band gap of the overlayer.

Au was deposited by a commercial MVD-source (Oxford Applied Research) from a carbon crucible filled by pieces of high purity (99.95%) metal. A commercially available SAES alkali getter source was used for K-deposition.

3. Results and discussion

3.1. Preparation and characterization of different supports: clean, K-predosed and Ar⁺-pretreated TiO₂(110) surfaces

TiO₂(110)-(1 × n) support showed characteristic added rows running in the [001] direction (Fig. 1A). The one-dimensional outrising rows randomly separated by n * 0.65 nm with a characteristic length of 15–20 nm can be attributed to epitaxially grown reduced titania rows (probably Ti₂O₃ phase) [30–34]. The mean height of these features was 0.11 nm. The interrow areas can be identified as (1 × 1) terraces [6]. It is worth mentioning that the orientation of the detected regions is the same for all images presented here. The surface concentration of the added rows (or added dots) varied only slightly during the experiments and in order to keep their amount constant it was necessary from time to time to reoxidize the surface in 5 × 10⁻⁴ mbar oxygen at 900 K for a few minutes. Accordingly, we can conclude that the surface studied here was substantially (1 × 1) bulk terminated TiO₂(110).

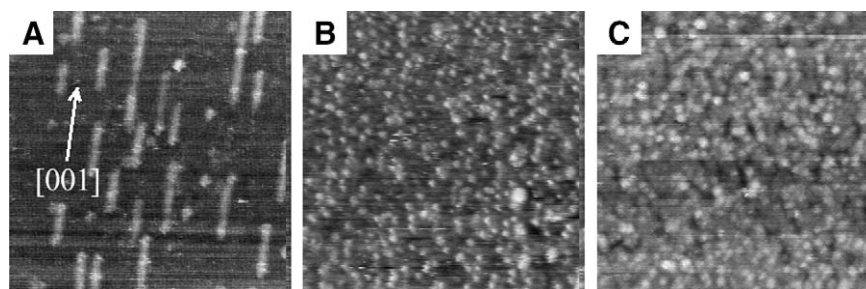


Fig. 1. Characteristic STM images of $50 \times 50 \text{ nm}^2$ recorded on (A) clean $\text{TiO}_2(110)$ surface, (B) deposited by 0.05 ML of K and (C) Ar^+ bombarded (0.5 keV) with flux of $1.25 \times 10^{14} \text{ Ar}^+ \text{ cm}^{-2} \text{ s}^{-1}$ for 10 min (that is $7.5 \times 10^{16} \text{ Ar}^+ \text{ cm}^{-2}$).

By deposition of K on the surface described above only dot-like features of a diameter of 1.25 nm and a height of 0.25 nm were detected (Fig. 1B). It is important to remark that the average corrugation calculated on the total area ($50 \times 50 \text{ nm}^2$) is approximately the same as for the clean surface (0.6 nm). In this case the coverage of the alkali ad-metal was approximately 0.05 ML which was estimated on the basis of the relative AES intensity ($R_K = 0.14$). R_K is defined as the ratio of the peak-to-peak intensity of K(KLL) AES signal at 252 eV and that of Ti(LMM) signal at 382 eV. The variation of the K coverage in the different experiments was followed by measuring R_K defined above. It was found that this ratio achieves a value of 2.80 at saturation of K near room temperature (330 K) and is assigned to 1 ML or to $5 \times 10^{14} \text{ K-atom cm}^{-2}$ density. By using the realistic assumption that the value of R_K is proportional to K coverage, R_K was used for the calibration of the surface concentration of K deposited on the $\text{TiO}_2(110)$ surface.

The ion-induced reduction of the $\text{TiO}_2(110)$ surface was carried out by Ar^+ bombardment. For this treatment a kinetic energy of 500 eV and ion density of $1.25 \times 10^{14} \text{ ion cm}^{-2} \text{ s}^{-1}$ were applied for 10 min. The result of the bombardment was checked by taking characteristic STM images at room temperature. Fig. 1C shows an area of $50 \times 50 \text{ nm}^2$ recorded on the bombarded $\text{TiO}_2(110)$ surface. It can be seen that the surface exhibits dot-like features similar to the case of K deposition described above. Several pit-like structures were also observed with an average length and depth of 5.20 nm and 0.15 nm, respectively. Nevertheless, the change of the average corrugation of the surface was not remarkable. These results are in good agreement with our detailed study on the effect of Ar^+ bombardment published earlier [35].

3.2. Deposition of Au on clean $\text{TiO}_2(110)$ surface at room temperature and the effect of annealing in UHV

Fig. 2 shows a series of STM images recorded on (A) clean, (B) Au deposited (at 320 K) and subsequently annealed $\text{TiO}_2(110)$ surfaces at different temperatures (C – 500 K, D – 700 K, E – 900 K, F – 1100 K) for 2 min. The size of the images is $50 \times 50 \text{ nm}^2$. Because of the 3D growth mode (Volmer–Weber) and the low intensity of

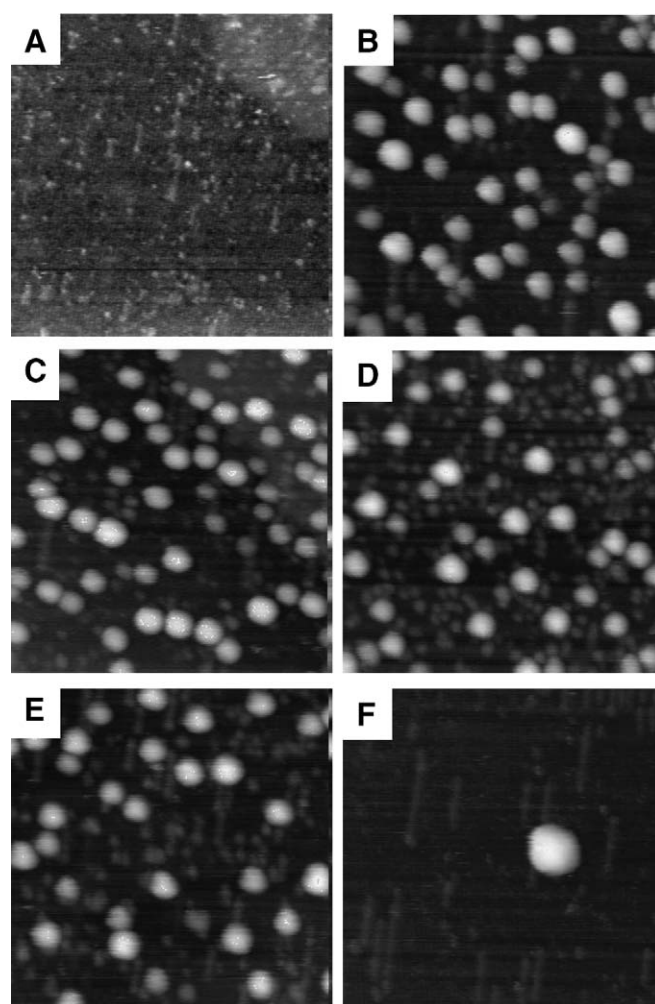


Fig. 2. STM images ($50 \times 50 \text{ nm}^2$) of (A) clean $\text{TiO}_2(110)$ surface, (B) deposited by 0.46 ML Au at 320 K and annealed at different temperatures for 2 min: (C) 500 K, (D) 700 K, (E) 900 K, (F) 1100 K.

the Au(LMM) AES signal, it was not possible to determine the surface coverage by Auger-electron spectroscopy. Instead, the volume of Au clusters calculated from the STM images was used for the calibration of the amount of Au deposited on the surface. This method can correctly be used when 3D growth mode manifests clearly [36]. The calculation is consisted of the following steps: (i) identification of the geometric form (hemispherical, coin, cubic,

hexagonal, etc. shape) of the particles; (ii) determination of the average size of the crystallites or categorization those in to size groups; (iii) calculation of the summarized volume of the particles for an average region of certain extension (usually $100 \times 100 \text{ nm}^2$ in our case); (iv) determination of the admetal coverage assuming of close packed particles. The clean $\text{TiO}_2(110)$ substrate exhibits only characteristic elongated string-like features and nanodots. In this case the corrugation of the surface is only 0.6 nm (Fig. 2A). The deposition of Au at near room temperature (320 K) results in the formation of 3D coin shape particles with a diameter of 3–4 nm and a height of 1–1.4 nm (Fig. 2B). It is worth mentioning that the rate of Au deposition was kept at constant value (ca. 0.3 ML min^{-1}) during the experiments presented below. The calculation of the total volume of the nanoparticles and the estimation of the amount of surface Au gave a value of 0.46 ML. Although this estimation for the concentration of deposited Au contains some error, by taking into account the different factors (size measurement, image noise, reproducibility for different sample regions) it is probably less than 20–30%. The annealing of this surface at elevated temperatures in the range of 500–700 K led to only a slight change in the overall morphology (Fig. 2C and D). The total volume and the average size of the Au adparticles changed only slightly in this temperature range (see also below in Fig. 4). The thermal treatments performed in UHV at higher temperatures (1100 K), however, caused a significant change of these parameters (Figs. 2F and 4A). In Fig. 2F it can be seen that only one particle is present in a $50 \times 50 \text{ nm}^2$ region (the smallest size representative area in this case), the diameter of which is approximately 5–6 nm. This behaviour can be explained by the so called Ostwald-ripening or the coalescence of the nanoparticles. At the same time the total volume of the surface gold decreased gradually between 900 K and 1100 K by at least 60–70% of the original value (Fig. 4A). This latter observation suggests that the ripening or coalescence processes are accompanied by the sublimation of Au from the surface in this higher temperature range.

3.3. The effects of predeposition of K and the prebombardment by Ar^+ on the formation and thermal stability of Au deposited on $\text{TiO}_2(110)$ surface

In the subsequent experiments STM images were recorded after the deposition of approximately 0.40 ML ($\pm 0.05 \text{ ML}$) Au on three different $\text{TiO}_2(110)$ substrates as described above (Section 3.1): (A) clean bulk terminated (1×1) surface; (B) the same surface following K exposure of 0.05 ML (surface concentration of $2.5 \times 10^{13} \text{ K atom cm}^{-2}$); (C) $\text{TiO}_2(110)(1 \times 1)$ surface reduced by 0.5 keV Ar ions with a flux of $1.25 \times 10^{14} \text{ cm}^{-2} \text{ s}^{-1}$ for 10 min. The deposition of Au was performed in each case in the temperature range of 320–330 K and the samples were annealed at 500 K and 700 K for 2 min (Fig. 3). It is worth mentioning that the annealing was continued at

even higher temperatures, but the morphology was quite similar in the three cases. For a better comparison, the size of all of the images shown in Fig. 3 is $20 \times 20 \text{ nm}^2$. Nevertheless, it is important to emphasize that the images of this small size are not entirely representative for the distribution of the particles, accordingly, larger images were statistically evaluated to draw the following statements. In the case of the clean $\text{TiO}_2(110)$ surface (A) the size and the distribution of the Au nanoparticles do not change substantially with thermal treatments at 500 K and 700 K, as it was already demonstrated above by STM images of $50 \times 50 \text{ nm}^2$ (Fig. 2C and D). The initial average diameter of 4–5 nm was determined for the Au nanoparticles formed during the deposition at 320 K and this parameter did not change on the effect of annealing (Fig. 3A). For the K-precovered surface (B) the deposition of Au resulted in particles with an average diameter of approximately 2.5 nm, seemingly smaller than in the case of the clean $\text{TiO}_2(110)$ substrate (Fig. 3B). Although the annealing at 500 K did not cause any appreciable change of this parameter, the annealing at 700 K resulted in larger particles of 3–4 nm and in a reduced surface concentration. In the case of the Ar^+ treated $\text{TiO}_2(110)$ surface (C) the deposition of Au led to the formation of nearly the same size particles (approximately 2.5 nm) similarly to the former case, however, the size distribution did not change on the effect of the subsequent thermal treatments (Fig. 3C). The change of the substantial morphological properties are depicted in Fig. 4 for the different cases, where graph A exhibits the total volume of the nanoparticles appeared after the different treatments in the temperature range of 300–1100 K, the graph B shows the mean size (atom content) of the Au particles between 300 K and 700 K. It is worth to remark that the estimated error of the vertical axis is approximately 20–30%, as it was previously mentioned. In all three cases the Au content of the surface changes only moderately in the temperature range of 300–700 K. The amount of Au seems to decrease significantly above 700 K (Fig. 4A). The number of Au atoms contained in the clusters formed at 320 K exhibits a sharp difference for the three cases: approximately four times more Au atoms constitute the particles on the clean $\text{TiO}_2(110)$ than on the K-precovered surface. This difference is slightly less on the effect of annealing, although even after annealing at 700 K the average size of the Au nanoparticles is greater by approximately 50% in the case of the clean $\text{TiO}_2(110)$ surface. It is seen clearly that the lowest particle size can be achieved on the K-precovered surface, although the thermal resistance of these particles is not very high.

Parallel with the investigations of the morphology of the clusters, systematic tunnelling spectroscopic measurements were also performed in the different states of the sample treatments. Although it was not possible to take I - V spectra in atomically resolved manner, some characteristic features were found by recording spectra on the top of the nanoparticles during the subsequent treatments (see Section 3.5).

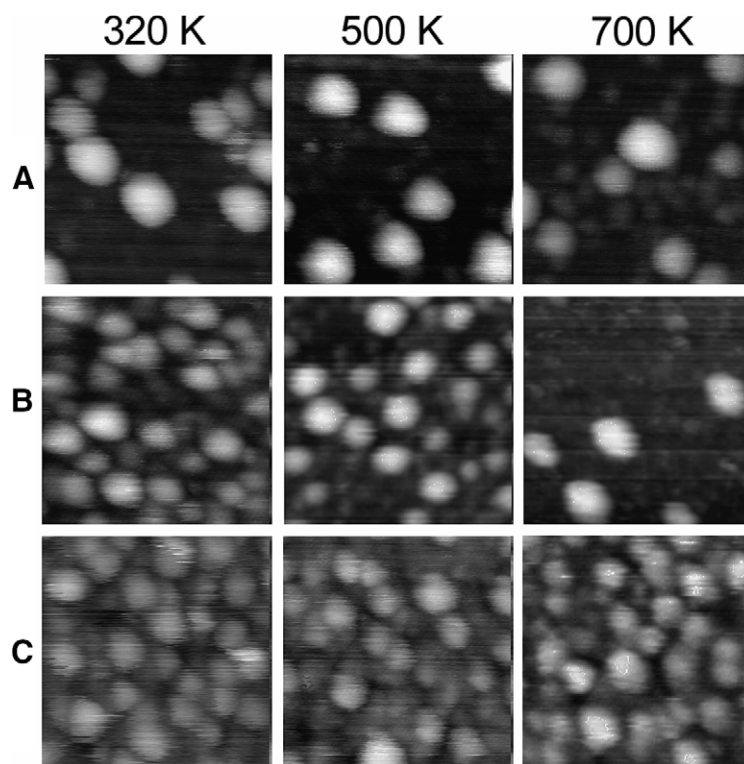


Fig. 3. Deposition of $0.40 (\pm 0.05)$ ML of Au at 320 K on three different surfaces: (A) clean $\text{TiO}_2(110)$ surface; (B) predeposited by 0.05 ML of K and (C) prebombarded by Ar^+ (0.5 keV, $7.5 \times 10^{16} \text{ Ar}^+ \text{ cm}^{-2}$). The effect of annealing of the prepared surfaces at 500 K and 700 K for 2 min. Image size: $20 \times 20 \text{ nm}^2$.

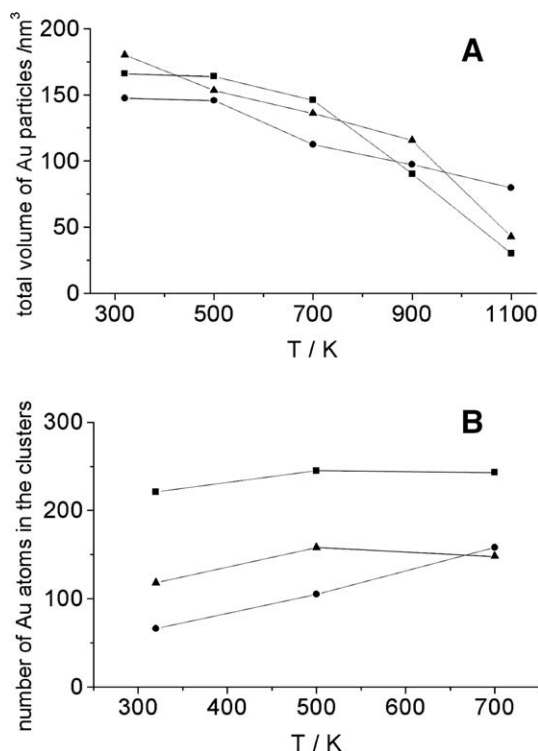


Fig. 4. (A) The total volume of the Au nanoparticles and (B) the number of Au atoms in an average nanocluster calculated from the STM images recorded on $50 \times 50 \text{ nm}^2$ surface area for the three different surfaces presented in Fig. 3: surf-A – ■; surf-B – ●; surf-C – ▲.

Former photoelectron spectroscopy studies revealed a relatively weak bonding to the stoichiometric TiO_2 surfaces resulting in only a small shift of the characteristic atomic orbitals of Ti and O [11,19,20,37,38]. The recent results obtained by scanning atom probe techniques (STM, AFM) have shown the formation of relatively large metal clusters ($>3\text{--}5 \text{ nm}$) even at room temperature, similarly as in the present work [11–16]. For the morphological characterization of thicker Au films (1–50 ML – monolayer equivalent) deposited at room temperature on $\text{TiO}_2(110)$ single crystal high resolution scanning electron microscopy was also successfully applied indicating an epitaxial relationship of $(111)\text{Au} \parallel (110)\text{TiO}_2$ with $[110]\text{Au} \parallel [001]\text{TiO}_2$ [17,18]. In a recent work Maeda et al. demonstrated clearly that on non-stoichiometric $\text{TiO}_2(110)$ -cross linked (1×2) surface the Au nanoparticle size distribution shifted toward the lower sizes compared to the case of stoichiometric (1×1) surfaces [16]. The prebombardment of $\text{TiO}_2(110)$ surface by Ar ions (0.5 keV, $10 \mu\text{A cm}^{-2}$, 10 min) followed by deposition of Au resulted also in an appreciable decrease of the average size of the Au nanoparticles [17]. These phenomena can obviously be explained by the experimental results obtained for the early stage of the formation of Au nanoparticles – experiments performed at very low admetal coverages and low temperatures (130–300 K) on atomic scale – where it was found that the oxygen vacancy sites strongly activate the nucleation of surface Au, moreover, the formation of Au–O–vacancy complex was assumed to

influence effectively the growth of Au nanoparticles [13,14]. This latter observation is also supported by DFT calculations [13,39–41]. The island growth kinetics during the vapour deposition of gold onto $\text{TiO}_2(110)$ at low temperatures has been examined also by low energy ion scattering (LEIS) and the experimental data were used for a detailed analysis of the surface diffusion properties [37].

In our study the effect of the deposition of K may be understood by assuming of the formation of surface oxygen defect sites which increases the concentration of Au seeds and stabilize the small sizes. The importance of the subsurface oxidation state was shown also for K/ TiO_2 system as long as the formation of detectable amount of Ti^{3+} species in XPS spectra was sensitively changed for stoichiometric and non-stoichiometric samples [25]. Atomic scale studies by STM and AFM methods were also performed in several cases for alkali metal atoms adsorbed on TiO_2 surfaces [27,28,42]. The main conclusion of these papers is in harmony with the earlier SEXAFS measurements and the theoretical calculations, namely, K bonds in the threefold hollow site formed by two bridging and one inplane oxygen atoms of the substrate lattice and results in a 1D zigzag structure running in the [001] direction.

3.4. Effects of the K coverage on the formation and thermal stability of the deposited Au

In this series of experiments the initial coverage of K was systematically varied in order to find the optimal K

precoverage for keeping the Au clusters in the possible smallest size. In this case somewhat less Au (0.15 ML) was deposited on the K-covered $\text{TiO}_2(110)$ surface as previously (Section 3.3) in order to obtain more separated Au nanoparticles and to measure their size. The corresponding STM images of $20 \times 20 \text{ nm}^2$ are presented in Fig. 5 where three differently K precovered (A – 0.15 ML, B – 0.60 ML, C – 1.80 ML) surfaces were exposed to Au at 320 K and annealed at 500 K and 700 K for 2 min. It can be seen that the lowest size of the Au nanoparticles was measured at near room temperature, just after the Au evaporation. The images show clearly that the average size of the Au particles decreases by increasing the K precoverage. At the same time it is also obvious that the K adlayer does not increase the thermal stability of the Au nanoparticles of small sizes. On the contrary, the surface potassium of higher coverage ($\theta_K = 0.62$) causes a dramatic agglomeration of the gold resulting in large (8–10 nm) and well separated Au particles (Fig. 5C). It should be mentioned that these latter images are not characteristic any more on the overall distribution of the Au particles, because of their small size ($20 \times 20 \text{ nm}^2$). In order to present the average distribution of gold, larger size images of $100 \times 100 \text{ nm}^2$ are shown in Fig. 6. This figure makes it possible to compare the large scale morphology of the Au-decorated clean and K precovered ($\theta_K = 0.62$, $R_K = 1.82$) $\text{TiO}_2(110)$ surfaces after deposition of Au at 320 K and after the subsequent annealing at 700 K (2 minutes) in UHV. It can be seen that for the K-covered surface the thermal treatment resulted in 3–4

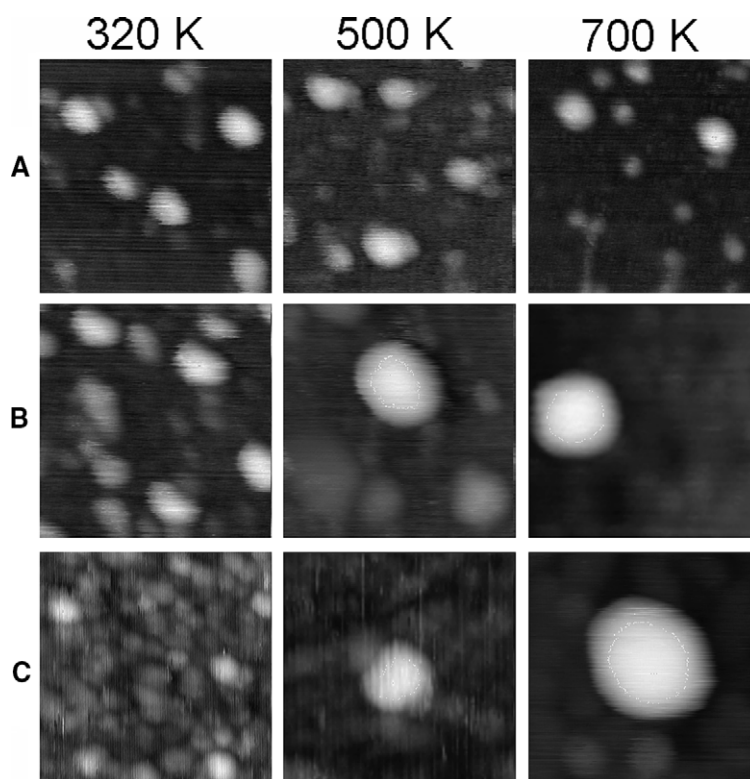


Fig. 5. The effect of K predosed at 320 K on the thermal stability of Au (0.15 ML) deposited at 320 K and annealed at 500 K and 700 K for 2 min: (A) $\theta_K = 0$; (B) $\theta_K = 0.08$; (C) $\theta_K = 0.62$. Image size: $20 \times 20 \text{ nm}^2$.

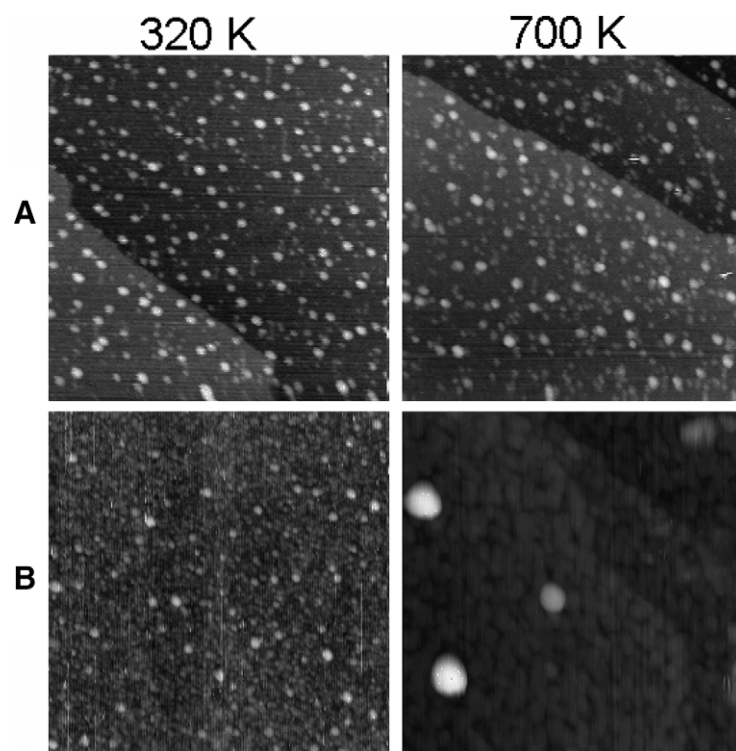


Fig. 6. The same experimental results as in Fig. 5 on larger scale of $100 \times 100 \text{ nm}^2$: deposition of gold at 320 K on (A) clean and (B) K precovered ($\theta_K = 0.62$) $\text{TiO}_2(110)$ surfaces and followed by annealing at 700 K for 2 min in UHV.

nanoparticles of 8–10 nm in a surface area of $100 \times 100 \text{ nm}^2$. The fine texture of the terraces in this latter case corresponds to the morphology detected for a K-covered surface treated in the same manner but Au deposition. A more detailed study on the K/ $\text{TiO}_2(110)$ system is under execution in our laboratory.

An excellent work published recently and dealing with the thermal induced sintering of Au deposits studied by a variable temperature movie-STM has shown that above 873 K the evaporation of gold from the $\text{TiO}_2(110)$ substrate competes with the Ostwald-ripening process [15]. This conclusion is in harmony with the observation presented here. One crucial question of our results above, how can the surface potassium activate the agglomeration of the adsorbed gold. It can be assumed that the formation of large Au clusters needs an enhanced surface diffusion of gold. This additional driving force can be supplied by an exothermic surface ordering of the potassium, i.e. formation of potassium oxide islands with a very low surface free energy.

3.5. Characterization of the different Au nanoparticles by tunnelling spectroscopy

In this section some tunnelling spectroscopy (I – V) curves are presented which were taken on the top of Au nanoparticles formed in the different treatments described in the previous sections (Fig. 7). It is important to remark that the spectra presented below are representatives of the

curves taken on numerous particles obtained in the same procedure. In Fig. 7A and B two I – V curves can be seen for a smaller and a larger Au particle of $d = 3.5 \text{ nm}$ and $d = 6.2 \text{ nm}$, respectively. The smaller particle was obtained after deposition of gold at room temperature, the larger one was produced by annealing the Au-covered surface at 1100 K. Both spectra exhibit electron states at the Fermi level (the slope of the curves are 10 pA/V and 312 pA/V at 0 V bias) indicating that the metal–non-metal transition of the Au nanoparticles takes place at the size less than approximately 3 nm. Moreover, this result also exhibits that the Au particles annealed at high temperature preserve their metallic properties. Comparing these curves to the I – V spectra recorded on a site of $\text{TiO}_2(110)$ terrace (Fig. 7C), it is clear that in the case of the oxide surface there is no electron states at the Fermi level (no measurable slope at 0 V bias). The most surprising result was obtained on the Au particles formed on K-covered and Au-deposited surfaces annealed at 700 K (Fig. 7D). In this case the size of the Au particle was nearly the same (6.5 nm) as for the clean support annealed at 1100 K, however, it exhibited a non-metallic behaviour, namely an extended zero current region at the Fermi level (0 pA/V slope). This property can be explained by several causes: (i) activated oxidation of the gold particles; (ii) the encapsulation of the Au nanoparticles by an oxide phase (K_xO or TiO_x); (iii) formation of an insulating sub-layer between the Au particle and the TiO_2 support. The oxidation of Au nanoparticles can certainly be excluded by thermodynamic reasons, however,

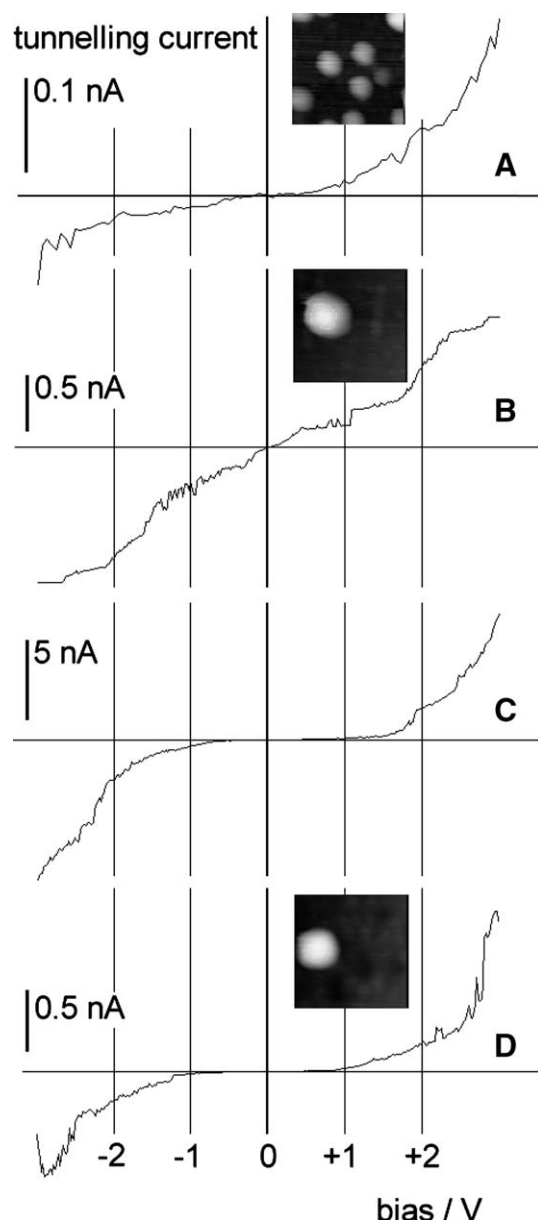


Fig. 7. Tunnelling spectroscopy spectra recorded on differently prepared Au nanoparticles: (A) on the particle (3.7 nm of diameter) formed by deposition of 0.45 ML of Au at 320 K; (B) on the top of an Au nanoparticle 6.7 nm formed on the same surface after annealing at 1100 K for 2 min; (C) characteristic I - V spectrum recorded above a clean $\text{TiO}_2(110)$ atomic terrace; (D) on the Au nanoparticle (6.1 nm) formed by deposition of Au (0.15 ML) on a $\text{TiO}_2(110)$ surface predeposited by K ($\Theta_K = 0.08$) and subsequent annealing at 700 K in UHV. The size of the images inserted: $20 \times 20 \text{ nm}^2$.

it is more difficult to distinguish between the two latter cases. It is worth mentioning that the decoration of the supported Pt nanoparticles by a reduced phase of titania is a well known phenomenon when the support is sufficiently reduced [43]. Similarly, it can be assumed that the surface potassium reduces the top layer of the titania support causing the decoration of the Au nanoparticles [21]. Unfortunately, the sensitivity of the Auger spectroscopy was not sufficient to make an unambiguous conclu-

sion for this process. Accordingly, to explain this interesting observation for I - V curves needs a further detailed study.

4. Conclusions

The formation of self organized nanoparticles on the solid surfaces is a complex process which is determined both by the thermodynamic properties as well as by the kinetics of the surface diffusion. The surface additives can induce some change of both factors. The technologically important Au/ $\text{TiO}_2(110)$ system provides an excellent model material for this type of study. It is also helpful for the explanation of the experimental results obtained in this study that many details of the bonding of K and Au atoms on the $\text{TiO}_2(110)$ surface were experimentally and theoretically discussed in the previous papers (see the references). The results presented here confirm the earlier observations for the stronger bonding of Au atoms on the oxygen deficient TiO_2 surface resulting in larger dispersity of the gold adlayer. Oxygen vacancies can be created both chemically by predeposition of K or physically by bombarding the surface by low energy Ar ions. It was shown that the mean size of Au nanoparticles can be decreased at room temperature by the pretreatment of the $\text{TiO}_2(110)$ surface by low energy Ar ions and also by the predeposition of K. Depending on the Au coverage the average size of the gold nanoparticles can be decreased from 4 to 5 nm to 2–3 nm on the pretreated $\text{TiO}_2(110)$ supports. At the same time, the K precoverage (approximately 0.5 ML) accelerates the growth of gold in to well separated large particles of 8–10 nm on the effect of the annealing at 700 K in UHV. This latter phenomenon may be interpreted by an increased surface mass transport connected to the exothermic restructuring of the K-adlayer itself. These properties suggest a rather complex morphological and a chemical influence of the K additive layers applied in the heterogeneous catalysis. On the basis of our results, it is obvious that the surface potassium is not only a chemical modifier but it has a strong effect on the morphology (structural modifier) of the catalytic metal nanoparticles supported on different oxide surfaces.

Acknowledgement

This work was supported by the Hungarian Scientific Research Fund (OTKA) through T43057 and T32040 projects, by the Hungarian Ministry of Education (NKFP-3A058-04, TET-CZ 09/04 and KNRET-07/2006).

References

- [1] M. Haruta, Catal. Today 36 (1997) 153.
- [2] C.J. Zhong, J. Luo, M.M. Maye, L. Han, N. Kariuki, in: B. Zhou, S. Hermans, G.A. Somorjai (Eds.), Nanotechnology in Catalysis, vol. 2, Kluwer Academic/Plenum Publishers, 2003, p. 221.
- [3] B. Schumacher, Y. Denkwitz, V. Plzak, M. Kinne, R.J. Behm, J. Catal. 224 (2004) 449.

- [4] F. Solymosi, T. Bánsági, T. Süli-Zakar, *Phys. Chem. Chem. Phys.* 5 (2003) 4724.
- [5] M.S. Chen, D.W. Goodman, *Catal. Today* 111 (2006) 22.
- [6] U. Diebold, *Surf. Sci.* 578 (2005) 1.
- [7] N. Lopez, T.V.W. Janssens, B.S. Clausen, Y. Xu, M. Mavrikakis, T. Bligaard, *J. Catal.* 223 (2004) 232.
- [8] C.T. Campbell, *Surf. Sci. Rep.* 27 (1–3) (1997) 1.
- [9] C.R. Henry, *Surf. Sci. Rep.* 31 (1998) 231.
- [10] U. Diebold, *Surf. Sci.* 48 (2003) 53.
- [11] S. Kielbassa, M. Kinne, R.J. Behm, *J. Phys. Chem. B* 108 (2004) 19184.
- [12] A. Kolmakov, D.W. Goodman, *Catal. Lett.* 70 (2000) 93.
- [13] E. Wahlström, N. Lopez, R. Schaub, P. Thosttrup, A. Rønneau, C. Africh, E. Lægsgaard, J.K. Nørskov, F. Besenbacher, *Phys. Rev. Lett.* 90 (2) (2003) 26101.
- [14] B.K. Min, W.T. Wallace, D.W. Goodman, *Surf. Sci.* 600 (2006) L7.
- [15] C.E.J. Mitchell, A. Howard, M. Carney, R.G. Egdell, *Surf. Sci.* 490 (2001) 196.
- [16] Y. Maeda, T. Fujitani, S. Tsubota, M. Haruta, *Surf. Sci.* 562 (2004) 1.
- [17] L. Zhang, F. Cosandey, R. Persaud, T.E. Madey, *Surf. Sci.* 439 (1999) 73.
- [18] F. Cosandey, L. Zhang, T.E. Madey, *Surf. Sci.* 474 (2001) 1.
- [19] S. Lee, C. Fan, T. Wu, S.L. Anderson, *J. Am. Chem. Soc.* 126 (2004) 5682.
- [20] S. Lee, C. Fan, T. Wu, S.L. Anderson, *Surf. Sci.* 578 (2005) 5.
- [21] P.J. Hardman, R. Casanova, K. Prabhakaran, C.A. Muryn, P.L. Wincott, G. Thornton, *Surf. Sci.* 269/270 (1992) 677.
- [22] K. Prabhakaran, D. Purdie, R. Casanova, C.A. Muryn, P.J. Hardman, P.L. Wincott, G. Thornton, *Phys. Rev. B* 45 (12) (1992) 6969.
- [23] R. Heise, R. Courths, *Surf. Sci.* 331–333 (1995) 1460.
- [24] A.G. Thomas, P.J. Hardman, C.A. Muryn, H.S. Dhariwal, A.F. Prime, G. Thornton, E. Román, J.L. de Segovia, *J. Chem. Soc., Faraday Trans.* 91 (20) (1995) 3569.
- [25] R. Lindsay, E. Michelangeli, B.G. Daniels, M.n. Polcik, A. Verdini, L. Floreano, A. Morgante, J. Muscat, N.M. Harrison, G. Thornton, *Surf. Sci.* 547 (2003) L859.
- [26] R. Lindsay, E. Michelangeli, B.G. Daniels, M.n. Polcik, A. Verdini, L. Floreano, A. Morgante, G. Thornton, *Surf. Sci.* 566 (2004) 921.
- [27] C.L. Pang, C.A. Muryn, A.P. Woodhead, H. Raza, S.S. Haycock, V.R. Dhanak, G. Thornton, *Surf. Sci.* 583 (2005) L147.
- [28] J. Muscat, N.M. Harrison, *Phys. Rev. B* 59 (23) (1999) 15457.
- [29] T. Bredow, E. Aprà, M. Catti, G. Pacchioni, *Surf. Sci.* 418 (1998) 150.
- [30] A. Berkó, A. Magony, J. Szökő, *Langmuir* 21 (2005) 4562.
- [31] S. Fischer, A. Munz, K.-D. Schierbaum, W. Göpel, *Surf. Sci.* 337 (1995) 17.
- [32] I.D. Cocks, Q. Guo, E.M. Williams, *Surf. Sci.* 390 (1997) 119.
- [33] R.A. Bennett, P. Stone, N.J. Price, M. Bowker, *Phys. Rev. Lett.* 82 (19) (1999) 3831.
- [34] S. Takakusagi, K.I. Fukui, F. Nariyuki, Y. Iwasawa, *Surf. Sci.* 523 (2003) L41.
- [35] A. Berkó, T. Bíró, T. Kecskés, F. Solymosi, *Vacuum* 61 (2001) 317.
- [36] A. Berkó, G. Ménesi, F. Solymosi, *Surf. Sci.* 372 (1997) 202.
- [37] S.C. Parker, A.W. Grant, V.A. Bondzie, C.T. Campbell, *Surf. Sci.* 441 (1999) 10.
- [38] A. Howard, D.N.S. Clark, C.E.J. Mitchell, R.G. Egdell, V.R. Dhanak, *Surf. Sci.* 518 (2002) 210.
- [39] Y. Wang, G.S. Hwang, *Surf. Sci.* 542 (2003) 72.
- [40] N. Lopez, J.K. Nørskov, *Surf. Sci.* 515 (2002) 175.
- [41] L. Giordano, G. Pacchioni, T. Bredow, J.F. Sanz, *Surf. Sci.* 471 (2001) 21.
- [42] P.W. Murray, N.G. Condon, G. Thornton, *Surf. Sci.* 323 (1995) L281.
- [43] A. Berkó, I. Ulrich, K.C. Prince, *J. Phys. Chem. B* 102 (1998) 3379.